diversity

MDPI

Article

Florpyrauxifen-Benzyl Drives Dose- and Time-Dependent Changes in the Structure and Function of Fungal Communities in Rice Rhizosphere Soil by Modulating Soil Physicochemical Properties

Chunguang Liu [1], Zongyang Zhang [1], Haiyan Fu [1], Xinyu Song [1], Bo Tao [2,*] and Fengshan Yang [1,*]

[1] Engineering Research Center of Agricultural Microbiology Technology, Ministry of Education & Heilongjiang Provincial Key Laboratory of Ecological Restoration and Resource Utilization for Cold Region & Key Laboratory of Microbiology, College of Heilongjiang Province & School of Life Sciences, Heilongjiang University, Harbin 150080, China; 2005013@hlju.edu.cn (C.L.)
[2] College of Agriculture, Northeast Agricultural University, Harbin 150030, China
* Correspondence: botaol@163.com (B.T.); yangfengshan@hlju.edu.cn (F.Y.)

Abstract

Herbicides are critical for ensuring food production and improving agricultural yields; however, their residues may alter soil ecology and pose risks to animals, plants, and humans via bioaccumulation. Florpyrauxifen-benzyl is a novel herbicide, and existing studies have mainly focused on its weed control efficacy, crop safety, and general environmental impacts. However, the effects of its application on soil fungal diversity remain poorly understood. To elucidate the degradation pathways of florpyrauxifen-benzyl and its impacts on soil microorganisms, this study employed liquid chromatography and high-throughput sequencing to analyze florpyrauxifen-benzyl residues, shifts in soil physicochemical properties, and alterations in soil fungal communities following herbicide application, thereby revealing the interactions between florpyrauxifen-benzyl and soil fungi. Our results showed that, compared with the untreated control, the 10-fold recommended dose significantly increased the relative abundances of *Pseudeurotium bakeri* and *Phialophora cyclaminis*. Furthermore, the fungal diversity indices in the 5-fold and 10-fold recommended dose groups were significantly higher at later sampling stages than those in both the untreated control and the recommended-dose groups. After florpyrauxifen-benzyl application, the core fungal communities in the treatment groups were markedly distinct from those in the untreated control. These findings provide guidance for the safe and rational use of florpyrauxifen-benzyl, and offer a theoretical framework and scientific basis for the ecological monitoring of soil contamination and the elucidation of herbicide degradation mechanisms.

Keywords: florpyrauxifen-benzyl; northeast rice soil; fungal; residual dynamics

Academic Editor: Ipek Kurtboke

Received: 6 July 2026
Revised: 11 September 2026
Accepted: 12 September 2026
Published: 19 September 2026

1. Introduction

Long-term application of herbicides may lead to substantial residue accumulation in soil and water. Florpyrauxifen-benzyl, as a newly developed herbicide, exerts its herbicidal efficacy by interfering with plant growth and development; upon binding to its target site, it disrupts normal physiological processes, resulting in plant malformation and eventual death. It is primarily absorbed by foliage, with a small fraction taken up by roots, and translocated via vascular tissues to accumulate at growing points, thereby killing target weeds. However, reports on its environmental fate, including residues and metabolism,

remain limited. Consequently, the development of analytical detection methods has become a major research focus.

Miller et al. [1] evaluated the effects of soil moisture on the uptake, translocation, and metabolism of florpyrauxifen-benzyl in three problematic weed species. They found that under moist conditions (60% soil water content), weed uptake of florpyrauxifen-benzyl was greater than that under low-moisture conditions. At 7.5% soil moisture, no significant differences in translocation were observed across the three weed species. In *Sesbania cannabina*, 95% of the recovered herbicide existed in the acid form under high soil moisture conditions, indicating that soil moisture modulated the content of the acid metabolite detected in this weed species. Tu Wangmancuo et al. [2] identified the major hydrolysis product of florpyrauxifen-benzyl as florpyrauxifen-acid using liquid chromatography-mass spectrometry. Pot incubation experiments showed that the metabolite florpyrauxifen-acid was detected in various matrices of the paddy field ecosystem as early as 2 h after application, and that the degradation rates of florpyrauxifen-benzyl and its metabolite florpyrauxifen-acid in the paddy environment exceeded 90% at 28 days after treatment. Zhou Rendan et al. [3] developed an analytical method for the determination of the active ingredient in 3% florpyrauxifen-benzyl emulsifiable concentrate, using ultra-performance liquid chromatography coupled with quadrupole linear ion trap time-of-flight mass spectrometry.

Herbicides exert substantial impacts on soil microorganisms and soil physicochemical properties. As key drivers of soil material transformation, soil microorganisms and physicochemical properties mediate the decomposition of soil organic matter and nutrient conversion, and are therefore widely recognized as core indicators for soil health assessment [4]. Du et al. [5] investigated the effects of metsulfuron-methyl on soil biodegradation capacity and nitrogen transformation, and found that the nitrogen cycle in both tested soils was slightly affected by metsulfuron-methyl. Liu et al. [6] studied the impacts of atrazine applications on soil aggregates, soil organic carbon, and tourmaline-associated soil proteins, and reported that soil organic carbon (SOC) content in soil aggregates was significantly negatively correlated with the duration of atrazine application. Chavez-Ortiz et al. [7] evaluated the effects of glyphosate and its commercial formulations on soil C, N, and P dynamics, and demonstrated that pure glyphosate exerted stronger effects on soil C and P kinetics than its commercial formulations.

Previous studies have also characterized the shifts in microbial diversity induced by different herbicides. A study by Zhou examined the effects of pyroxsulam on soil enzyme activities, the expression of nitrogen and carbon cycling-related genes, and bacterial community structure. The results showed that pyroxsulam altered the dominant phyla and functional bacterial genera associated with soil nitrogen and carbon cycling, and increased the relative abundance of bacterial genera capable of suppressing soil-borne diseases and degrading organic pollutants [8]. Ma et al. [9] investigated the effects of long-term exposure to the herbicide nicosulfuron on bacterial community structure in agricultural soils, and found that prolonged nicosulfuron exposure increased the α-diversity and relative abundance of bacteria and archaea, whereas the relative abundances of *Bacteroidetes* and *Acidobacteria* were significantly reduced compared with soils free of nicosulfuron residues. Ghosh et al. [10] assessed the impacts of long-term atrazine application on soil enzyme activities and bacterial community structure, and observed that atrazine significantly increased the relative abundance of Actinobacteria. Lv et al. [11] investigated the effects of different concentrations of chlorimuron-ethyl on soil microbial communities in Sesbania rhizosphere soil. Their results indicated that low chlorimuron-ethyl concentrations significantly enhanced the diversity and richness of soil microbial communities, while high concentrations exerted inhibitory effects.

To date, studies worldwide have mainly focused on aspects including weed control efficacy, herbicide compatibility, safety and phytotoxicity to current and succeeding crops, soil adsorption and translocation, responses of aquatic plants, and impacts on soil bacterial communities [12,13]. However, the effects of florpyrauxifen-benzyl residues on soil fungal community structure remain poorly understood, and the ecological roles and potential responsiveness of soil fungal communities have not yet been fully elucidated. To clarify the disturbance patterns of florpyrauxifen-benzyl on soil fungi and evaluate the associated soil ecological risks, this study was conducted using black paddy soil from Northeast China in an outdoor pot incubation system. The soil was sieved to remove crop residues, and the sampled paddy field had no prior history of microbial inoculation. Using high-performance liquid chromatography (HPLC), titration colorimetry, and high-throughput sequencing, we analyzed florpyrauxifen-benzyl residues in paddy soil and their impacts on soil physicochemical properties and fungal community structure, aiming to elucidate the residual dynamics of florpyrauxifen-benzyl in paddy soil and its effects on soil properties and fungal communities. We hypothesized that florpyrauxifen-benzyl application would exert significant effects on soil physicochemical properties and fungal community structure. The findings of this study will provide a theoretical basis for clarifying the disturbance patterns of florpyrauxifen-benzyl on soil fungi, mitigating soil-borne diseases in crop roots, and preventing soil microecological imbalance.

2. Materials and Methods

2.1. Soil Sampling

Soil samples were collected from a paddy field in Harbin, Heilongjiang Province, China (46.00° N, 126.64° E) for use in a rice pot experiment. The experiment was conducted at the pot experimental facility of the College of Life Sciences, Heilongjiang University, Harbin, Heilongjiang Province (45.71° N, 126.62° E). This region is located in the second accumulated temperature zone, with an annual precipitation of 800 mm and an annual accumulated temperature of 2500–2700 °C. The soil type in this area is black loam, with no prior history of microbial inoculation. In the previous 3–5 years, the major crop grown was the locally dominant rice cultivar Wuyoudao No. 1. The soil was air-dried at room temperature to a constant weight, then ground and passed through 40-mesh and 60-mesh sieves. The sieved soil was collected, homogenized, and stored for subsequent use.

2.2. Experimental Design

The test herbicide florpyrauxifen-benzyl, a foliar-applied herbicide, was sprayed at the rice seedling stage when plants reached the two-leaf and one-heart stage. The experimental period lasted 30 days after herbicide application, covering the entire rice tillering stage. A total of four treatments were set for potted rice plants. The florpyrauxifen-benzyl formulation used in this study was a 3% emulsifiable concentrate (EC), purchased from Corteva (Johnston, IA, USA). According to global field application guidelines, the recommended field rates of florpyrauxifen-benzyl active ingredient range from 5 to 50 g a.i. ha^{-1}, depending on crop type, weed density, and weed growth stage. Three herbicide treatments were employed: F1 at 5 g a.i. ha^{-1}, F5 at 25 g a.i. ha^{-1}, and F10 at 50 g a.i. ha^{-1}. An untreated control group (F0) with no florpyrauxifen-benzyl application was also included.

The pot experiment was arranged as follows: each pot (12 cm × 12 cm × 28 cm) was filled with 2 kg of paddy soil. A total of 48 pots were assigned across the four treatments. Soil sampling was performed at 1, 5, 15, and 30 days after herbicide application, with three replicate pots sampled per treatment at each time point. For each pot, fresh soil from the 0–10 cm top layer was collected via a three-point sampling method and thoroughly mixed

to form a single composite sample per pot [14]. This experiment adopted a destructive sampling strategy.

2.3. Determination of Florpyrauxifen-Benzyl Residues in Soil

Extraction of florpyrauxifen-benzyl from soil samples was performed as follows. Briefly, 5 g of soil sample was placed in a 50 mL centrifuge tube, and 15 mL of extraction solvent (hexane/acetone, 1:1, *v*/*v*) was added. The suspension was subjected to ultrasonication for 5 min and then centrifuged at 5000 rpm for 5 min. The supernatant was transferred to a glass tube, and the extraction procedure was repeated three more times (four extraction cycles in total). The supernatants from all cycles were combined and evaporated to dryness under a gentle nitrogen stream. The residue was reconstituted in 2 mL of methanol with ultrasonication for 30 s, and then passed through a 0.22 μm membrane filter followed by a C18 solid-phase extraction (SPE) cartridge for purification [15].

Florpyrauxifen-benzyl was quantified using ultra-performance liquid chromatography (UPLC; Waters ACQUITY H-Class UPLC system) [16]. The optimized chromatographic conditions were set as follows: Waters ACQUITY UPLC BEH C18 column (1.7 μm particle size, 2.1 mm × 50 mm); detection wavelength, 230 nm; column temperature, 40 °C; flow rate, 0.30 mL/min; mobile phase, acetonitrile/water (3:1, *v*/*v*); injection volume, 3 μL. The retention time was 2.916 ± 0.05 min.

To validate the reliability of the soil extraction procedure and chromatographic conditions, recovery tests were performed by spiking florpyrauxifen-benzyl into both soil and water matrices at three concentrations (0.05, 0.5, and 5.0 mg/kg), with three replicates for each concentration. Soil without florpyrauxifen-benzyl spiking served as the blank control. The recovery rate of florpyrauxifen-benzyl was calculated as the ratio of the measured concentration to the spiked concentration. The coefficient of variation (CV) was defined as the ratio of the standard deviation to the mean recovery.

5.00 mg of florpyrauxifen-benzyl reference standard was accurately weighed and dissolved in chromatographic-grade methanol in a 10 mL volumetric flask, and the volume was made up to the mark with the same solvent. The solution was filtered through a 0.45 μm organic-phase membrane filter, and the filtrate was used as the 500 mg/L standard stock solution, which was sealed and stored for subsequent use. A series of florpyrauxifen-benzyl working solutions were prepared by diluting the stock solution with methanol to final concentrations of 0.05, 0.1, 0.5, 1, 1.5, and 2 mg/L. Calibration curves and linear regression equations were established based on the linear relationship between standard solution concentrations and corresponding peak areas detected by UPLC, from which the quantitation equation for florpyrauxifen-benzyl in soil was derived. The residue dissipation curve of florpyrauxifen-benzyl was constructed, and the half-life of florpyrauxifen-benzyl in rice pot soil was calculated using Equations (1) and (2) [17].

$$C_t = C_0 e^{-kt} \quad (1)$$

$$t_{1/2} = \ln 2 / k \quad (2)$$

Note: C_t: residual concentration at time t in mg/L; C_0: initial concentration, in mg/L; $t_{1/2}$: half-life indays; k: dissolution rate constant.

2.4. Determination of Soil Physicochemical Properties

In this study, six soil physicochemical properties were determined for each soil sample, including total nitrogen (TN), total phosphorus (TP), total potassium (TK), soil organic matter (SOM), air-dried moisture content, and pH. Soil pH and air-dried moisture content were measured using a pH meter and a moisture tester, respectively [18]. Total nitrogen content

was quantified via sulfuric acid digestion followed by the Kjeldahl nitrogen determination method [19]. Total phosphorus content was determined by the sodium hydroxide fusion method coupled with the molybdenum-antimony ascorbic acid colorimetric method [20]. Total potassium content was measured using flame photometry [21]. Soil organic matter content was analyzed via the potassium dichromate volumetric method with external heating [22].

2.5. Soil High-Throughput Sequencing

Approximately 0.5 g of each potted soil sample was frozen in liquid nitrogen and stored at −80 °C for high-throughput sequencing. Soil samples were collected on days 1, 5, 15, and 30, with three biological replicates per treatment. Total genomic DNA was extracted from soil samples. Full-length primers targeting the eukaryotic 18S rRNA gene were synthesized: Euk-A (forward: 5′-AACCTGGTTGATCCTGCCAGT-3′) and Euk-B (reverse: 5′-GATCCTTCTGCAGGTTCACCTAC-3′). PCR amplification was performed in a total volume of 25 μL reaction system containing 12.5 μL of 2× Taq Plus Master Mix, 3 μL of BSA (2 ng/μL), 1 μL of each forward and reverse primer (5 μM), 2 μL of template DNA (30 ng), and 5.5 μL of ddH_2O. The PCR thermal profile consisted of an initial denaturation at 94 °C for 5 min; 30 cycles of denaturation at 94 °C for 1 min, annealing at 55 °C for 1 min, and elongation at 72 °C for 1 min; a final elongation step at 72 °C for 10 min; and a hold at 4 °C. Purification, quantification and normalization of PCR amplicons were carried out to construct SMRT-Bell sequencing libraries. After library quality assessment, qualified libraries were sequenced on the PacBio Sequel II platform. High-throughput sequencing was performed by Biomarker Technologies Co., Ltd. (Beijing, China; www.biocloud.net). Raw PacBio subreads were processed to generate circular consensus sequence (CCS) reads, followed by CCS filtering and chimera removal. Bioinformatic analyses included operational taxonomic unit (OTU) clustering, diversity analysis, differential taxa analysis, and correlation analysis.

2.6. Statistical Analysis

Raw subreads were generated from the PacBio Sequel II(Menlo Park, USA) sequencing platform and processed using SMRT Link v8.0 software. Circular consensus sequence (CCS) reads were obtained with the filtering criteria of minPasses $\geq$ 5 and minPredictedAccuracy $\geq$ 0.9. Barcode demultiplexing was performed using lima (v1.7.0) with default parameters. Subsequently, cutadapt (v2.7) was used to recognize and trim the terminal Euk-A/Euk-B primer sequences, allowing a 20% mismatch rate, and sequences without matched primers were discarded. Qualified sequences were further filtered according to fragment length, with a valid length range of 1200–2000 bp for 18S rRNA sequences. Chimeric sequences were removed using UCHIME (v8.1) [23], and the remaining high-quality sequences were used for subsequent bioinformatic analysis.

Operational taxonomic unit (OTU) clustering was performed using USEARCH v10.0 [24] with a 97% sequence similarity threshold. Low-abundance OTUs were filtered by removing taxa with a total relative abundance lower than 0.005% of all sequences [25]. Taxonomic annotation of high-quality sequences was conducted using QIIME 2 (v2020.6). The 18S rRNA sequences were annotated against the Silva database (Release 138) [26], with additional reference to the NCBI RefSeq Targeted Loci database to improve annotation accuracy and comprehensiveness.

Taxonomic classification was performed using the classify-consensus-blast algorithm embedded in QIIME 2 (v2020.6). The algorithm screened the top three optimal alignment results to determine the consistent taxonomic classification, with the following default

thresholds: minimum sequence similarity of 90%, minimum query coverage of 90%, and minimum consensus confidence of 51%.

QIIME 2 (v2020.6) was applied to calculate the alpha diversity indices of soil eukaryotic microbial communities at the genus level. The Wilcoxon rank-sum test was used to evaluate differences in alpha diversity indices among different treatments. Beta diversity was analyzed to characterize spatial and temporal variations in community composition based on the binary Jaccard distance matrix. Permutational multivariate analysis of variance (PERMANOVA) was performed with 999 permutations to assess the statistical significance of community dissimilarity, and the corresponding F-statistic, coefficient of determination (R), and p-value were calculated. Note: R^2 represents the proportion of variance explained (calculated as $SS_{between}/SS_{total}$), $SS_{between}$ is the sum of squares between groups, SS_{total} is the total sum of squares, F is the test statistic, $df_{between}$ is the degrees of freedom among treatment groups, and $df_{residual}$ is the degrees of freedom within groups [27].

$$R^2 = \frac{SS_{between}}{SS_{total}} \tag{3}$$

$$F = \frac{SS_{between}/df_{between}}{SS_{residual}/df_{residual}} \tag{4}$$

FUNGuild (Fungi Functional Guild) was utilized for the functional annotation of fungal communities, which enables the taxonomic and ecological classification of massive sequencing datasets into functionally and ecologically meaningful categories [28]. Principal coordinate analysis (PCoA) was performed using R software (v4.4.1) to visualize and interpret the differences in fungal community structure among treatments.

Linear discriminant analysis effect size (LEfSe) analysis was conducted to screen biomarker taxa with significant differences in soil fungal communities under different herbicide treatments. Based on the OTU abundance matrix and taxonomic annotation table, the Kruskal–Wallis rank-sum test was applied to detect abundance variations of taxonomic units, with a linear discriminant analysis (LDA) threshold set at 4.0. The LDA score histogram and taxonomic cladogram were generated for visual presentation. For co-occurrence network analysis, datasets were grouped according to different herbicide treatments based on the genus-level fungal OTU abundance matrix. Low-abundance fungal genera with zero abundance in more than half of the samples within each group were preliminarily removed. The psych package in R was used to calculate pairwise Spearman's correlation coefficients among fungal genera at the genus level. The top 80 fungal genera in relative abundance were retained for network construction, with an edge number limit of 100. Only significant correlations with $r \geq 0.1$ and $p < 0.05$ were reserved. The node and edge files of each group were imported into Gephi v0.9.2, and the Fruchterman-Reingold layout algorithm was adopted for network visualization.

Canoco v5.0 software was used to analyze the correlations among herbicide treatments, soil fungal communities, and soil physicochemical properties. For all univariate indicators except alpha diversity indices, homogeneity of variance tests were performed first, followed by general linear model analysis and Duncan's multiple range test for pairwise comparisons. All statistical analyses were conducted using SPSS v26.0 (IBM Corporation, New York, NY, USA). Statistical significance was defined as follows: significant difference at $p < 0.05$, highly significant difference at $p < 0.01$, and extremely significant difference at $p < 0.001$.

3. Results

3.1. Residual Dynamics of Florpyrauxifen-Benzyl in Soil

Florpyrauxifen-benzyl application resulted in detectable residue accumulation in paddy soil, with residue concentrations increasing progressively with rising application

dosage. Residue concentrations in all treatment groups declined continuously over the 30-day experimental period. Across the four sampling time points (days 1 to 30), residues dissipated significantly faster in high-dose treatments than in low-dose treatments. As shown in Figure 1, the degradation curves of the F10, F5, and F1 treatments fitted well to the exponential decay function $C_t = C_0 e^{-kt}$, with R^2 values of 0.92, 0.88, and 0.84, respectively. Detailed kinetic parameters are provided in Table S1.

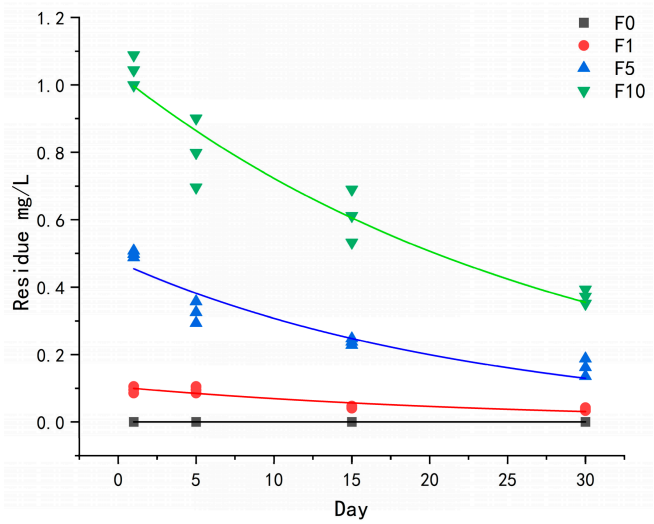

Figure 1. Residual Dynamics of florpyrauxifen-benzyl Soil. (n = 3, $p < 0.05$).

3.2. Effects of Florpyrauxifen-Benzyl Ester on Soil Physicochemical Properties

The temporal dynamics of soil physicochemical properties across all treatments over the incubation period are presented in Table S2. Soil total nitrogen, total phosphorus, organic matter, and pH all exhibited pronounced dynamic responses to both herbicide dosage and incubation time. The non-parallel response curves indicated an interaction effect between dosage and incubation time: the influence of florpyrauxifen-benzyl on soil physicochemical properties was not constant, but instead varied with incubation time.

In the untreated control group, soil physicochemical properties showed natural temporal fluctuations over the incubation period, whereas herbicide application altered the dynamics of nutrient transformation and release. Specifically, high-dose treatments significantly modulated soil nitrogen and phosphorus availability, organic matter decomposition, and soil acid-base status. Furthermore, the perturbation of soil physicochemical properties induced by florpyrauxifen-benzyl occurred predominantly in the early incubation stage (days 1 and 15), while differences among treatment groups gradually stabilized by day 30. These dynamic patterns are illustrated in Figure S1 and Table S2.

3.3. Effects of Florpyrauxifen-Benzyl on Fungal Community Structure in Rice Rhizosphere Soil

3.3.1. Effects of Florpyrauxifen-Benzyl on Fungal Species Composition in Soil

The ten dominant fungal phyla by relative abundance across all samples were *Ascomycota* (7.796–74.625%), *Chytridiomycota* (0.958–70.28%), *Mortierellomycota* (4.123–50.78%), *Basidiomycota* (1.39–33.13%), *Rozellomycota* (0.118–10.04%), *Blastocladiomycota* (0–1.24%), *Monoblepharomycota* (0–1.07%), *Glomeromycota* (0–1.02%), *Olpidiomycota* (0–0.76%), and *Aphelidiomycota* (0–0.36%). *Ascomycota* is the most species-rich phylum within the fungal kingdom.

Over the incubation period, the relative abundance of several phyla shifted significantly in the treatment groups: *Chytridiomycota*, *Glomeromycota*, and *Aphelidiomycota* showed notable increases, while *Ascomycota*, *Mortierellomycota*, *Rozellomycota*, *Blastocladiomycota*, and *Olpidiomycota* exhibited significant decreases. In contrast, the relative abundances of *Basidiomycota* and *Monoblepharomycota* did not change significantly over time ($p > 0.05$).

Compared with the untreated control, the relative abundance of *Ascomycota* in the F5 and F10 groups increased significantly on day 15, as did that of *Chytridiomycota* and *Glomeromycota* in the F10 group. By day 30, the relative abundances of *Monoblepharomycota* and *Blastocladiomycota* in the F10 group were significantly higher than those in the control ($p < 0.05$) (Figure 2A).

The ten dominant fungal genera by relative abundance were *Mortierella* (4.12–50.78%), *Phialophora* (0.38–16.47%), *Chaetomium* (1.02–13.51%), *Fusarium* (0.079–12.39%), *Botryotrichum* (0–10.19%), *Talaromyces* (0–8.32%), *Gelasinospora* (0–24.52%), *Aspergillus* (0–6.02%), *Penicillium* (0–5.42%), and *Discosia* (0–42.58%). Over time, significant increases in relative abundance were observed for *Botryotrichum* and *Aspergillus* in the treatment groups. Conversely, the relative abundances of *Mortierella*, *Phialophora*, *Chaetomium*, *Fusarium*, and *Penicillium* declined significantly. The abundances of *Talaromyces*, *Gelasinospora*, and *Discosia* did not change notably over time ($p > 0.05$).

Compared with the untreated control, the relative abundances of *Botryotrichum* and *Discosia* in the F1, F5, and F10 groups decreased significantly on day 5. On day 15, the relative abundance of *Botryotrichum* continued to decrease significantly across all treatment groups, while that of *Phialophora* and *Fusarium* in the F10 group increased significantly. By day 30, *Fusarium* and *Aspergillus* in the F10 group showed significant increases relative to the control (Figure 2B).

The ten dominant fungal species by relative abundance were *Mortierella rishikesha* (2.44–35.80%), *Phialophora cyclaminis* (0.38–16.47%), *Mortierella hyalina* (0.53–10.45%), *Mortierella sarnyensis* (0–13.27%), *Botryotrichum domesticum* (0–10.20%), *Talaromyces thailandensis* (0–24.37%), *Gelasinospora brevispora* (0–8.32%), *Discosia pseudoartocreas* (0–42.58%), *Pseudogymnoascus destructans* (0.078–3.93%), and *Pseudeurotium bakeri* (0–19.89%).

Over the incubation period, the relative abundance of *Botryotrichum domesticum* increased significantly in the treatment groups, while that of *Mortierella rishikesha*, *Phialophora cyclaminis*, *Mortierella hyalina*, and *Pseudogymnoascus destructans* decreased significantly. In contrast, the relative abundances of *Mortierella sarnyensis*, *Talaromyces thailandensis*, *Gelasinospora brevispora*, *Discosia pseudoartocreas*, and *Pseudeurotium bakeri* did not change significantly over time ($p > 0.05$).

Compared with the untreated control, the relative abundances of *Discosia pseudoartocreas* and *Botryotrichum domesticum* in the F1, F5, and F10 groups decreased significantly on day 5. On day 15, the relative abundance of *Mortierella rishikesha* in the F5 and F10 groups also declined significantly, while that of *Botryotrichum domesticum* continued to decrease across all three treatment groups. Additionally, the relative abundance of *Phialophora cyclaminis* in the F10 group increased significantly relative to the control (Figure 2C).

Compared with the untreated control group (F0), the F10 group showed higher relative abundances of *Kotlabaea*, *Cephalotrichum*, *Mortierella*, and *Neobulgaria* on day 1, and these genera exhibited highly similar abundance response patterns. On day 5, the relative abundances of *Aspergillus*, *Curvularia*, *Gelasinospora*, *Geotrichum*, *Cladosporium*, *Penicillium*, *Nigrospora*, *Sarocladium*, *Mrakia*, and *Pseudeurotium* were elevated in the F10 group, with these genera displaying highly consistent response patterns. On day 15, genera with increased relative abundances in the F10 group included *Fusarium*, *Cladosporium*, *Vishniacozyma*, *Zasmidium*, *Hyalocladosporiella*, *Occultifur*, *Wallemia*, *Pseudogymnoascus*, *Tausonia*, *Curvularia*, *Paraphaeosphaeria*, *Chaetomium*, *Gelasinospora*, *Mycofalcella*, Penicillium, and *Tricladium*, and these genera likewise showed highly similar abundance dynamics. On day 30, genera with higher relative abundances in the F10 group comprised *Condenascus*, *Monasus*, *Schizothecium*, *Aspergillus*, *Cladorrhinum*, *Mrakia*, *Glaciozyma*, *Podospora*, *Geotrichum*, *Cladosporium*, *Vishniacozyma*, *Fusarium*, *Humicola*, *Tausonia*, and *Trichocladium*, and these genera similarly presented highly consistent response patterns (Figure S2).

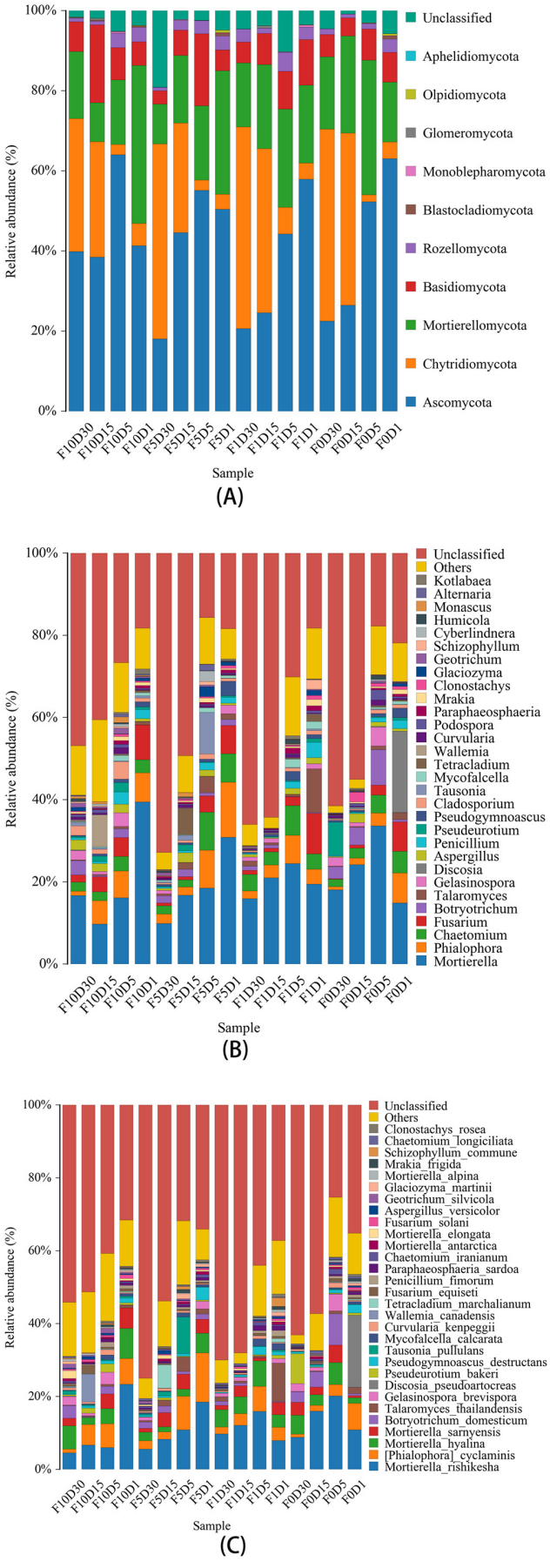

Figure 2. Histograms depicting the distribution of soil fungi at the phylum (**A**), genus (**B**), and species (**C**) levels under different treatment conditions. (n = 3, $p < 0.05$).

3.3.2. Effects of Florpyrauxifen-Benzyl on Soil Fungal Diversity

Alpha diversity reflects the species richness and evenness of individual microbial communities. The Shannon index is sensitive to both species richness and community evenness, while the Chao1 and ACE indices are standard estimators of species richness.

On day 15, compared with the untreated control (F0), the ACE and Chao1 indices in the F1 group were significantly decreased ($p < 0.01$ and $p < 0.05$, respectively), whereas the Chao1 index in the F5 group was significantly increased ($p < 0.01$). Additionally, the ACE index in the F5 group was significantly higher than that in the F1 group.

On day 30, the F10 group showed significant increases in the Shannon ($p < 0.05$), ACE ($p < 0.05$), and Chao1 ($p < 0.05$) indices compared with both the F0 control and the F5 group (Figure 3).

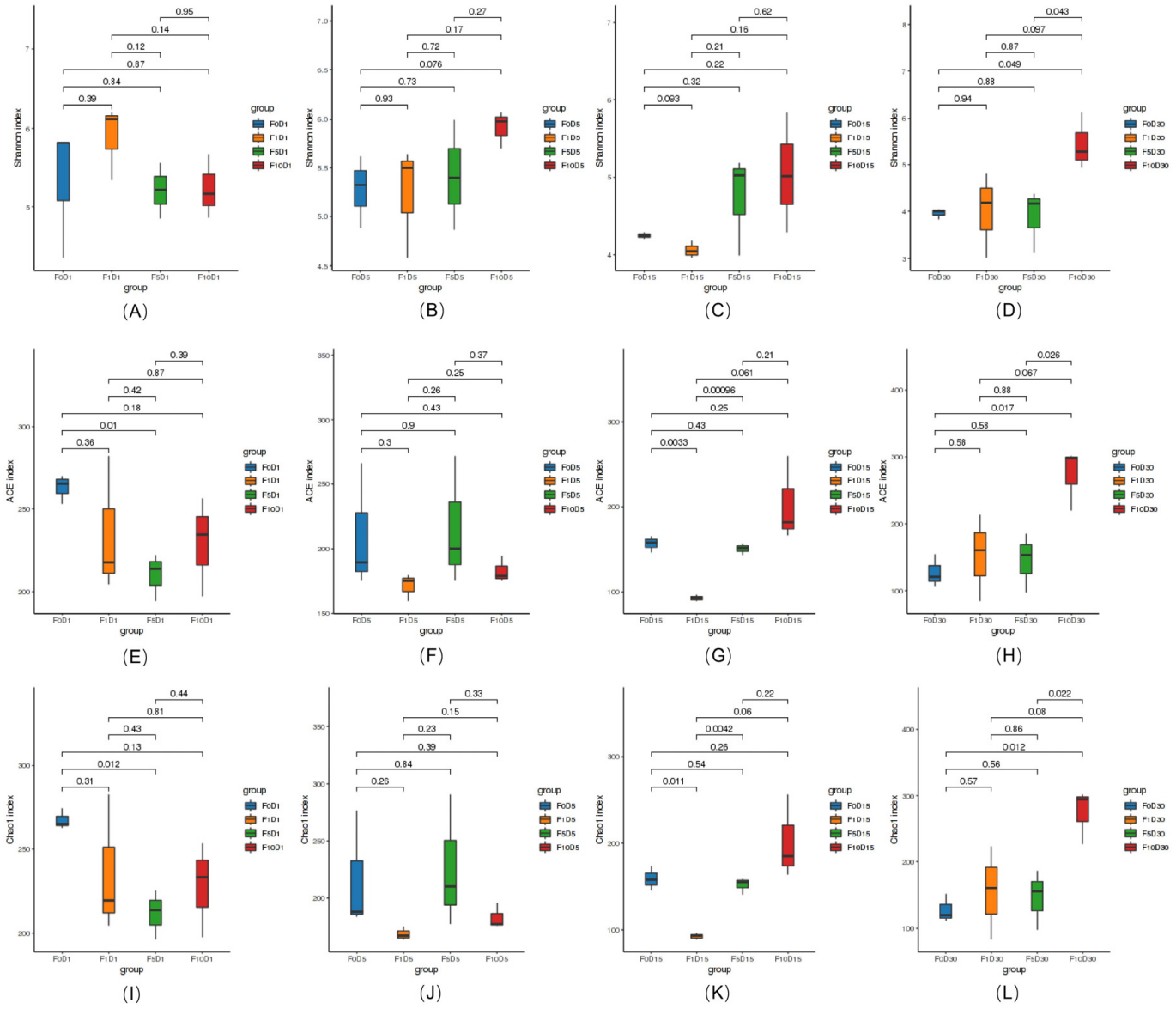

Figure 3. The impact of herbicides on intergroup differences in the alpha-diversity index of soil fungi. (n = 3, $p < 0.05$). Note: (**A**–**D**) Shannon; (**E**–**H**) ACE; (**I**–**L**) Chao1.

Rarefaction curves rose sharply before reaching a plateau, indicating that species richness did not increase significantly with further sequencing depth and that sequencing coverage was sufficient for subsequent data analyses (Figure S3A). Shannon index rarefaction curves rose sharply before leveling off, confirming that the sequencing data

volume was adequate and that increasing the number of sequencing reads would not lead to the detection of additional novel species (Figure S3B). Rank-abundance curves exhibited a relatively wide span, reflecting high community richness, while their relatively flat terminal segments indicated high evenness of species composition (Figure S3C). For the cumulative species discovery curves, the red curve showed a pattern of rapid initial increase followed by a plateau, indicating that a large number of new species were captured at the early sampling stage, while species richness did not increase significantly with expanding sample size. The green accumulation curve (derived from boxplot statistics) reflects the detection rate of common species. As sampling effort increased, the green curve first decreased and then stabilized, suggesting that the number of newly detected common species gradually diminished and approached saturation. This pattern confirmed that sampling effort was sufficient and that additional sampling was not required for robust data analysis (Figure S3D).

Principal coordinates analysis (PCoA) was applied to visualize differences in community composition among multiple groups on a two-dimensional ordination plot, where the two axes are derived to capture the maximum proportion of total variance in the distance matrix. The first principal coordinate (PC1) explained 17.78% of the total variation in fungal community composition, while the second principal coordinate (PC2) explained 8.95%. The results revealed clear spatial separation among the four groups—control (F0), low-dose (F1), medium-dose (F5), and high-dose (F10)—in the ordination space, indicating that florpyrauxifen-benzyl application significantly altered soil fungal community composition. Specifically, F0 samples clustered predominantly in the right region of the ordination plot; F1 samples aggregated mainly in the lower-left quadrant; and F5 and F10 samples concentrated in the upper-left quadrant, with partial overlap between the two higher-dose groups. The F0 control group was most clearly separated from all herbicide-treated groups. The community structures of F5 and F10 were relatively similar, with partial intermixing of samples between the groups. The F1 treatment group exhibited a larger confidence ellipse area, reflecting higher within-group dispersion and greater intra-group variability in community composition.

Overall, the distinct clustering patterns of samples from different treatment groups further confirm that florpyrauxifen-benzyl application altered the overall compositional structure of the soil fungal community, and that community composition shifted in a dosage-dependent manner (Figure 4).

In the PERMANOVA analysis, a larger R^2 value indicates a greater proportion of total variance explained by inter-group differences, reflecting more pronounced dissimilarities in fungal community composition among groups. A *p*-value below 0.05 indicates statistically significant inter-group differences. Based on Jaccard distance, no significant differences in fungal community composition were detected among the four groups on day 1 or day 5 ($p > 0.05$). In contrast, significant inter-group differences were observed on day 15 and day 30 ($p < 0.05$) (Figure 5).

As shown in the boxplots of inter-group β-diversity patterns, a βNTI value of <-2 or >2 represents a deviation of more than two standard deviations between the observed β mean nearest taxon distance (βMNTDobs) and the mean βMNTD derived from the null model (the expected level of phylogenetic turnover under random ecological processes), indicating that phylogenetic turnover is significantly lower or higher than the random expectation. Values of $|\beta NTI| < 2$ indicate that stochastic processes dominate community assembly, whereas values of $|\beta NTI| > 2$ indicate that deterministic processes are dominant.

On days 5, 15, and 30, βNTI values in the F1, F5, and F10 groups were significantly higher than those in the F0 control group. Across all four sampling time points (days 1, 5, 15, and 30), βNTI values for all groups (F0, F1, F5, and F10) fell within the range of -2 to

2, suggesting that fungal community assembly was mainly situated in the transition zone between deterministic and stochastic processes (Figure 6).

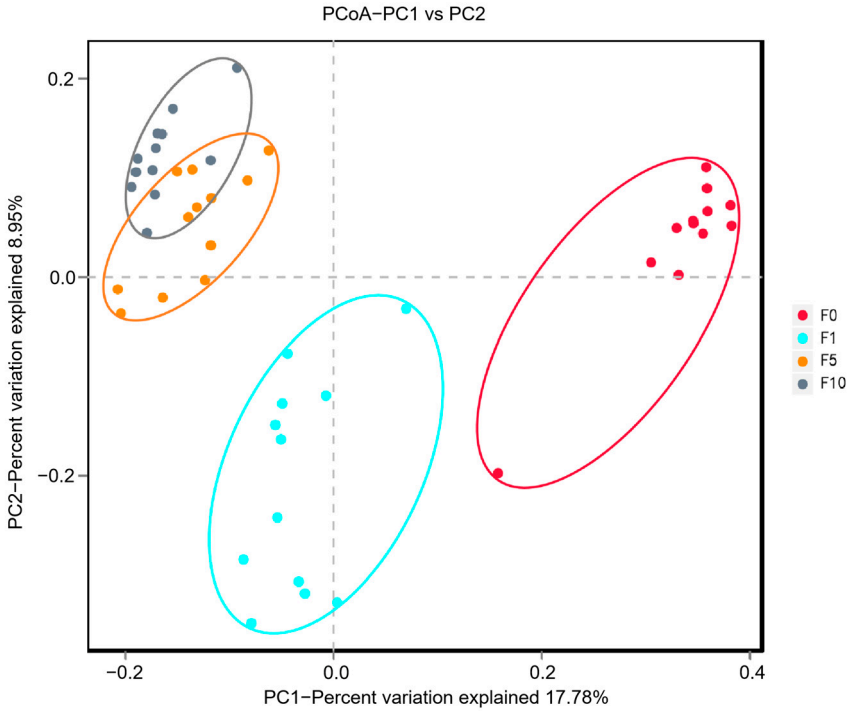

Figure 4. Two-dimensional plot of principal Coordinates Analysis (PCoA) for soil fungi OTUs following herbicide application. (n = 3, $p < 0.05$).

3.3.3. Significance Analysis of Fungal Community Differences in Soil Subjected to Florpyrauxifen-Benzyl

LEfSe analysis generates two main visualization outputs: a histogram of linear discriminant analysis (LDA) scores (Figure 7) and a taxonomic cladogram (Figure 8). The LDA score histograms revealed dynamic successional shifts in core fungal taxa across the four sampling time points, as detailed below:

In the F0 control soil, core fungal taxa shifted from class *Sordariomycetes* (order *Sordariales*, family *Sporocadaceae*), represented by *Discosia* and *Discosia pseudoartocreas*, at day 1, to taxa including order *Sordariales* and genera *Botryotrichum* and *Botryotrichum domesticum* at days 5 and 15. These were subsequently replaced by taxa such as *Clonostachys* (order *Hypocreales*) and members of family *Bionectriaceae* by day 30.

In the F1 treatment soil, core fungal taxa transitioned from class *Eurotiomycetes* (order *Eurotiales*), order *Hypocreales* (family *Nectriaceae*), genera *Fusarium* and *Talaromyces* (including *Talaromyces thailandensis*), as well as class *Leotiomycetes* (family *Trichocomaceae*) at day 1, to taxa including family *Helotiaceae*, class *Agaricomycetes*, genus *Penicillium*, and order *Agaricales* at intermediate time points, and finally to phylum *Chytridiomycota* by day 30.

In the F5 treatment soil, core fungal taxa across days 1–30 showed a continuous succession pattern: starting from family *Herpotrichiellaceae* and genera *Phialophora* and *Phialophora* cyclaminis at day 1, shifting to class Tremellomycetes, order *Cystofilobasidiales*, genus *Chaetomium*, family *Mrakiaceae*, order *Saccharomycetales*, class *Saccharomycetes*, order *Pleosporales*, and class *Microbotryomycetes* at intermediate stages, then to family *Aspergillaceae*, and finally to class *Lobulomycetes* by day 30.

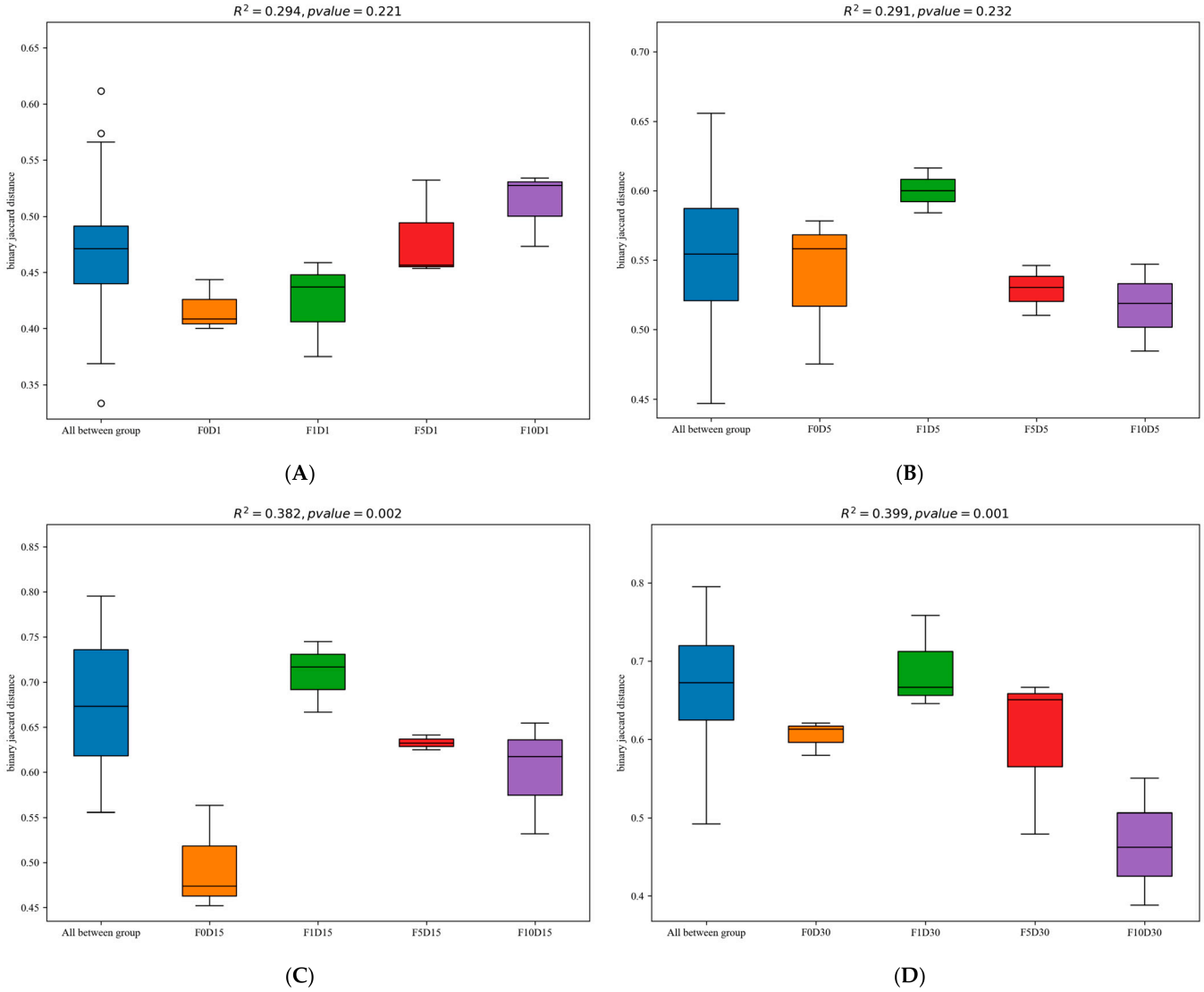

Figure 5. PERMANOVA inter-group analysis box plot for soil fungi following herbicide application. (n = 3, $p < 0.05$). Note: (**A**) day 1; (**B**) day 5; (**C**) day 15; (**D**) day 30.

In the F10 treatment soil, core fungal taxa shifted from class *Mortierellomycetes* (order *Mortierellales*, family *Mortierellaceae*, genus *Mortierella*), including *Mortierella rishikesha* and *Mortierella hyalina*, at days 1 and 5, to phylum *Ascomycota*, class *Dothideomycetes*, family *Cladosporiaceae*, order *Cladosporiales*, and genus *Cladosporium* at later time points (Figure 7).

Analysis of fungal phylogenetic lineages revealed distinct core fungal taxa across different sampling time points and treatment groups, with the distribution patterns clearly presented in the cladogram (Figure 8).

On day 1, core fungal taxa varied notably among the four treatment groups. In the F0 control group, core taxa ranging from class to species level included *Sordariomycetes*, *Sporocadaceae*, *Discosia*, and *Discosia pseudoartocreas*, all clustered within the same phylogenetic branch. In the F1 group, core taxa formed multiple distinct yet cohesive phylogenetic branches: one branch contained taxa from order to genus level (*Hypocreales*, *Nectriaceae*, and *Fusarium*), a second branch comprised taxa from family to species level (*Trichocomaceae*, *Talaromyces*, and *Talaromyces thailandensis*), and additional separate branches covered taxa from class to family level (*Leotiomycetes*, *Helotiales*, *Helotiaceae*), from class to genus level (*Eurotiomycetes*, *Eurotiales*, *Penicillium*), and from class to order level (*Agaricomycetes*, *Agaricales*). In the F5 group, core fungal taxa from family to species level (*Herpotrichiellaceae*, *Phialophora*,

and *Phialophora cyclaminis*) were grouped within the same phylogenetic branch. In the F10 group, core taxa spanning from phylum to species level (*Mortierellomycota*, *Mortierellomycetes*, *Mortierellales*, *Mortierellaceae*, *Mortierella*, and *Mortierella rishikesha*) all fell within a single phylogenetic branch.

On day 5, the composition of core phylogenetic lineages continued to shift across the different treatments. In the F0 group, core fungal taxa from order to species level (*Sordariales*, *Botryotrichum*, and *Botryotrichum domesticum*) were located on the same phylogenetic branch. In the F5 group, core fungal taxa formed adjacent phylogenetic branches, including taxa from class to family level (*Tremellomycetes*, *Microbotryomycetes*, *Cystofilobasidiales*, *Mrakiaceae*) and from class to order level (*Saccharomycetes*, *Saccharomycetales*). In the F10 group, core fungal taxa from phylum to genus level (*Ascomycota*, *Dothideomycetes*, *Cladosporiales*, *Cladosporiaceae*, and *Cladosporium*) clustered together on a single branch.

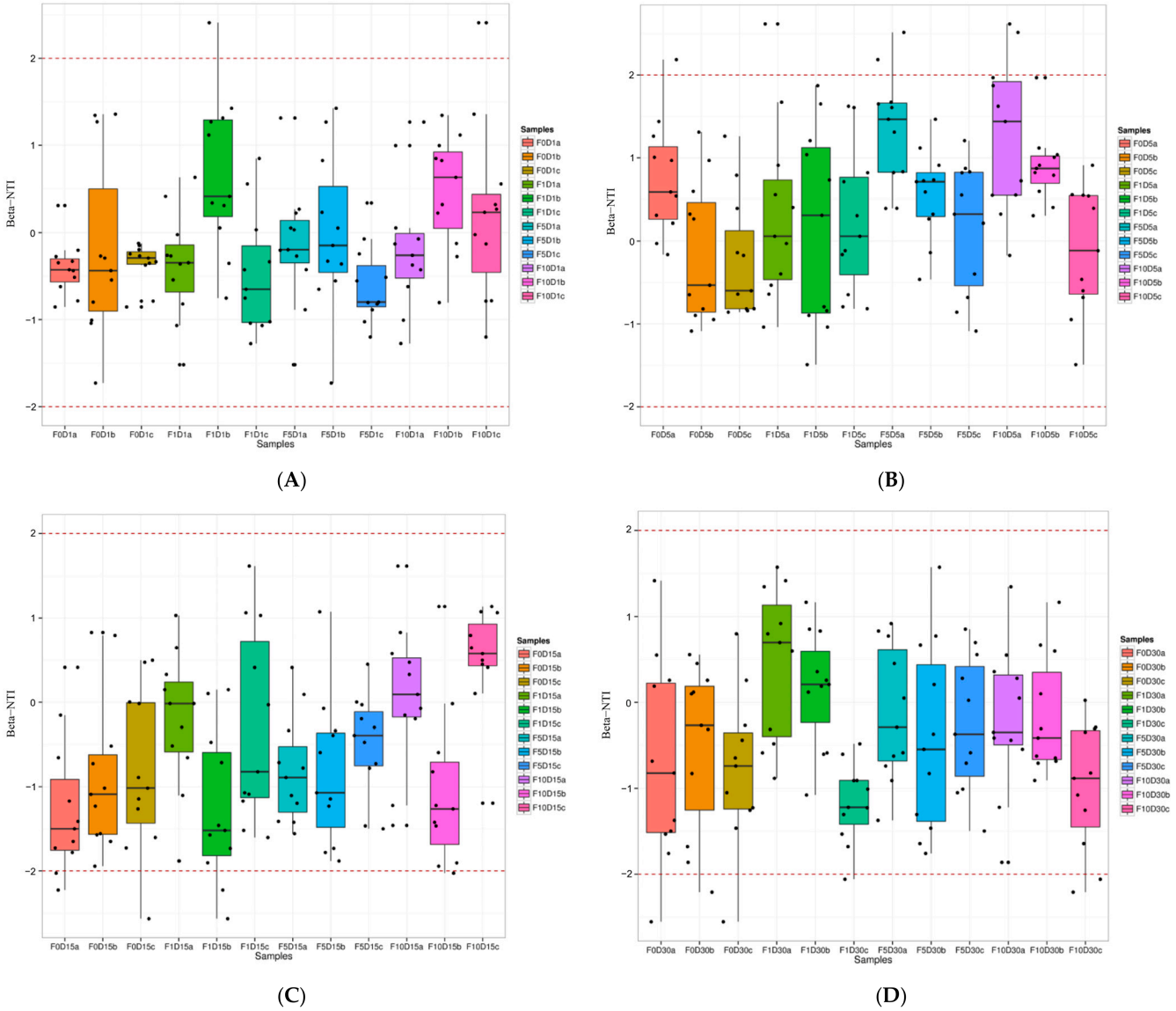

(**A**) (**B**)

(**C**) (**D**)

Figure 6. Box plot of soil fungal β-distance after application of different herbicides on the same date. (n = 3, $p < 0.05$). Note: (**A**) day 1; (**B**) day 5; (**C**) day 15; (**D**) day 30.

By day 15, the core phylogenetic lineages showed further successional changes. In the F0 group, core fungal taxa from family to genus level (*Bionectriaceae* and *Clonostachys*) were

grouped within the same phylogenetic branch. In the F5 group, core fungi were primarily represented by the family *Aspergillaceae*.

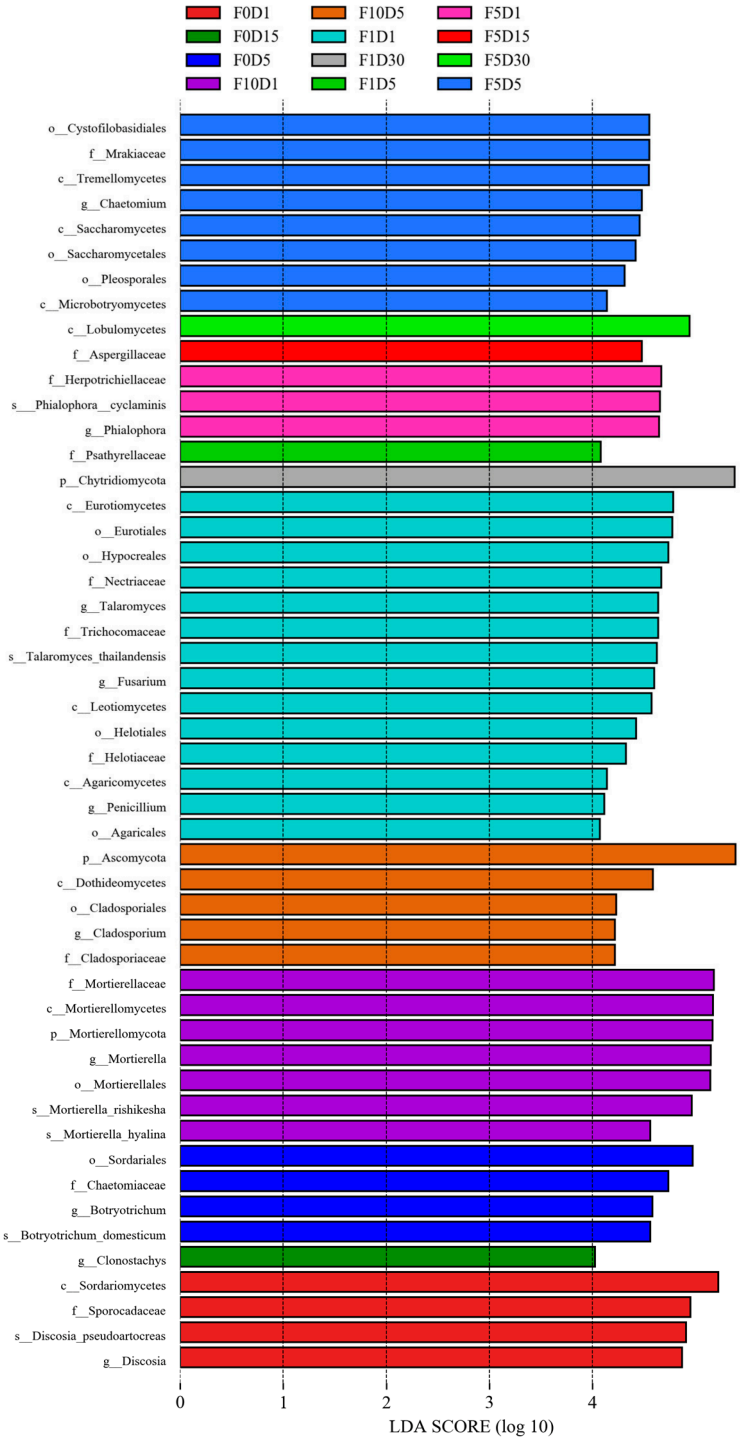

Figure 7. Histogram of LDA value distribution for soil fungi after herbicide application. (n = 3, $p < 0.05$).

By day 30, the core lineages presented clear differentiation among treatment groups. In the F1 group, the dominant fungal lineage belonged to the phylum *Chytridiomycota*. In the F5 group, core fungi were assigned to the class *Lobulomycetes*, forming a single phylogenetic branch.

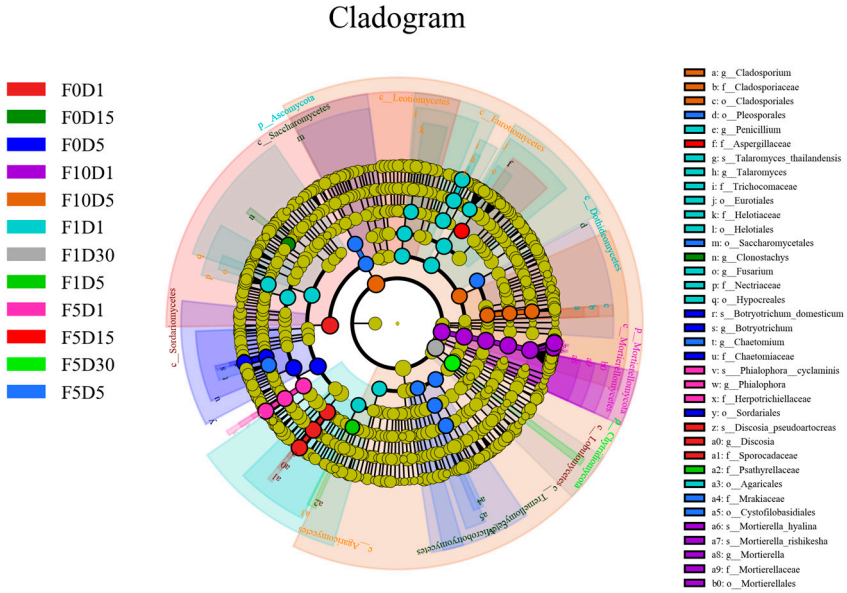

Figure 8. Fungal Phylogenetic Tree. (n = 3, $p < 0.05$).

3.3.4. Network Analysis of Soil Fungal Species Correlations Under Florpyrauxifen-Benzyl Treatment

Correlation network analysis was applied to investigate the interspecific interaction patterns of soil fungal communities. The genus-level correlation networks of fungal modules revealed that core taxa in the four treatment groups shifted notably over the 30-day incubation period.

In the F0 control group, 2 to 4 major network clusters were identified across the four sampling time points from day 1 to day 30. The core taxa of the network shifted from *Phialophora* and *Discosia* on day 1 to *Mortierella*, *Condenascus*, *Cladosporium*, and *Gelasinospora* by day 30. In the F1 treatment group, 3 to 4 major clusters were observed across the four time points. The core network taxa transitioned from *Mortierella*, *Talaromyces*, and *Chaetomium* on day 1 to *Phialophora*, *Gelasinospora*, *Mortierella*, and *Chaetomium* by day 30.

In the F5 treatment group, 2 to 4 major clusters were detected across the four sampling time points. The core taxa were initially dominated by *Chaetomium*, *Mortierella*, and *Phialophora* on day 1, fluctuated in composition on days 5 and 15, and returned to a core structure similar to that on day 1 by day 30. In the F10 treatment group, 2 to 4 major clusters were present across the four time points, with core taxa shifting from *Mortierella* and *Phialophora* on day 1 to *Mortierella*, *Botryotrichum*, and *Aspergillus* by day 30.

Analysis of genus-level correlation modules revealed distinct differences in core fungal taxa between the herbicide treatment groups and the untreated control at each corresponding sampling time point (Figure 9). On day 1, compared with the F0 control group, the F1 and F5 groups both had core fungal communities dominated by *Mortierella* and *Chaetomium*, while the F10 group was characterized by core taxa consisting of *Mortierella* and *Phialophora*. On day 5, the core communities of the F1 and F5 groups were mainly composed of *Chaetomium*, whereas the core fungal taxa in the F10 group had shifted to *Fusarium* and *Phialophora*. On day 15, the core genera in the F1 group included *Phialophora*, *Chaetomium*, and *Podospora*. The F5 group harbored core fungi represented by *Tetracladium*, *Aspergillus*, and *Talaromyces*, and the F10 group featured core taxa of *Phialophora*, *Chaetomium*, and *Zasmidium*. By day 30, the F1 and F5 groups still maintained core fungal communities dominated by *Phialophora* and *Chaetomium*, while the core taxa of the F10 group had shifted to *Botryotrichum* and *Aspergillus*.

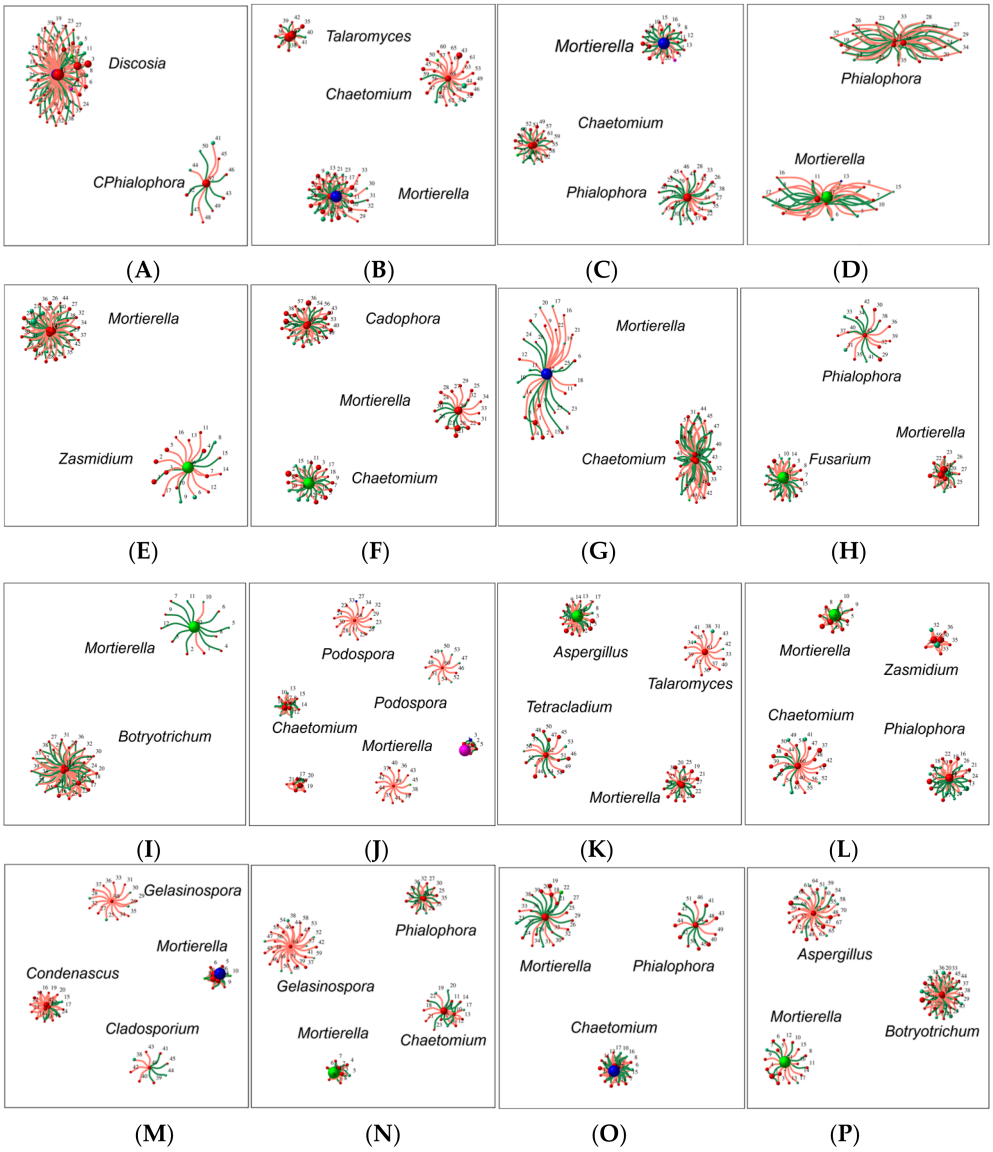

Figure 9. NICLY Module Correlation Network Diagram (n = 3, $p < 0.05$). Note: (**A**) F0 Day 1; (**B**) F1 Day 1; (**C**) F5 Day 1; (**D**) F10 Day 1; (**E**) F0 Day 5; (**F**) F1 Day 5; (**G**) F5 Day 5; (**H**) F10 Day 5; (**I**) F0 Day 15; (**J**) F1 Day 15; (**K**) F5 Day 15; (**L**) F10 Day 15; (**M**) F0 Day 30; (**N**) F1 Day 30; (**O**) F5 Day 30; (**P**) F10 Day 30.

The top five fungal genera with the highest species richness were *Phialophora*, *Chaetomium*, *Fusarium*, *Talaromyces*, and *Penicillium*. No negative *intergeneric* correlations were detected across the 36 analyzed fungal genera; instead, all pairs exhibited positive correlations. A positive correlation indicates that the abundance of one genus increases or decreases synchronously with that of another. The genus pairs showing the highest positive correlation coefficients included *Penicillium* and *Mycofalcella*, *Tetracladium* and *Volutella*, *Penicillium* and *Volutella*, *Fusarium* and *Mycofalcella*, *Fusarium* and *Glaciozyma*, *Conocybe* and *Glaciozyma*, *Fusarium* and *Phialophora*, *Penicillium* and *Chaetomium*, *Pseudogymnoascus* and *Phialophora*, and *Fusarium* and *Talaromyces*. The detailed correlation network is shown in Figure S4.

3.3.5. Functional Prediction Analysis of Soil Fungi Under Florpyrauxifen-Benzyl Treatment

FUNGuild is a widely applied tool for the ecological guild classification of fungi, providing a standardized and consistent framework to categorize taxa from large-scale sequencing datasets into ecologically meaningful functional groups. Fungi are assigned to three major nutritional modes: pathotrophs, which acquire nutrients by invading and damaging host cells; symbiotrophs, which obtain nutrition through mutualistic resource exchange with host cells; and saprotrophs, which gain nutrients by decomposing dead organic matter. These three primary nutritional categories are further subdivided into 12 detailed ecological guilds.

Taxonomic matching was performed against the built-in reference database of FUNGuild, with output records including species names, taxonomic ranks, nutritional modes, growth forms, morphological traits, and confidence levels. Only taxa with confidence levels classified as "Highly probable" or "Probable" were retained for visualization analysis; guild groups containing fewer than two qualifying taxa were excluded from the final visualization. In this study, the term "guild" refers to a functional grouping based on ecological resource utilization strategies rather than phylogenetic relatedness. These microecological guilds thus represent assemblages of fungi that share similar resource acquisition patterns within the soil environment. The relative abundances of pathotrophic, saprotrophic, and symbiotrophic fungi across all soil samples are presented in Figure S5.

The relative abundances of the three fungal nutritional modes across different dosage groups at each sampling time point are shown in Figure 10. On day 1 after florpyrauxifen-benzyl application, compared with the untreated F0 control, the relative abundance of saprotrophic fungi was significantly increased in the F1, F5, and F10 groups, while that of pathotrophic fungi was significantly decreased across all three treatment groups. The relative abundance of symbiotrophic fungi was significantly higher in the F10 group than in the F0 control. On day 5, no significant differences in the relative abundances of saprotrophic and pathotrophic fungi were detected among all groups; however, symbiotrophic fungi showed significantly higher relative abundances in the F1 and F5 groups relative to the control. On day 15, the abundances of saprotrophic and pathotrophic fungi remained comparable across all treatment groups, while the relative abundance of symbiotrophic fungi was significantly elevated in the F1 group compared with F0. By day 30, compared with the F0 control, the relative abundance of saprotrophic fungi was significantly decreased in the F1, F5, and F10 groups. Pathotrophic fungi exhibited a significantly increased relative abundance in the F10 group, and symbiotrophic fungi were significantly more abundant in both the F5 and F10 groups.

As shown in Figure S6, the relative abundances of the three fungal nutritional modes shifted dynamically over time following florpyrauxifen-benzyl application to soil. In the untreated F0 control group, the relative abundance of saprotrophic fungi increased significantly over the incubation period, while that of pathotrophic fungi decreased significantly. No significant temporal change was observed in the relative abundance of symbiotrophic fungi. In the F1 treatment group, the relative abundance of saprotrophic fungi exhibited a trend of initial decrease followed by subsequent increase over time, but the changes did not reach statistical significance. The relative abundance of pathotrophic fungi showed an increasing trend, but the differences were not statistically significant. The relative abundance of symbiotrophic fungi followed a trend of initial increase followed by decrease, and was significantly lower on day 30 than on day 5. In the F5 treatment group, the relative abundance of saprotrophic fungi showed a trend of initial decrease followed by increase over time, with no significant difference compared with the level on day 1. However, it was significantly higher on days 15 and 30 than on day 5. The relative abundance of pathotrophic fungi displayed a trend of initial increase followed by decrease over time, but

the differences were not statistically significant. The relative abundance of symbiotrophic fungi showed a trend of initial increase followed by decrease over time, with no significant differences across time points. In the F10 treatment group, the relative abundance of saprotrophic fungi fluctuated over time, but the changes did not reach statistical significance. The relative abundance of pathotrophic fungi also showed a fluctuating trend over time, with no significant differences. The relative abundance of symbiotrophic fungi exhibited a decreasing trend over time, but the changes were not statistically significant.

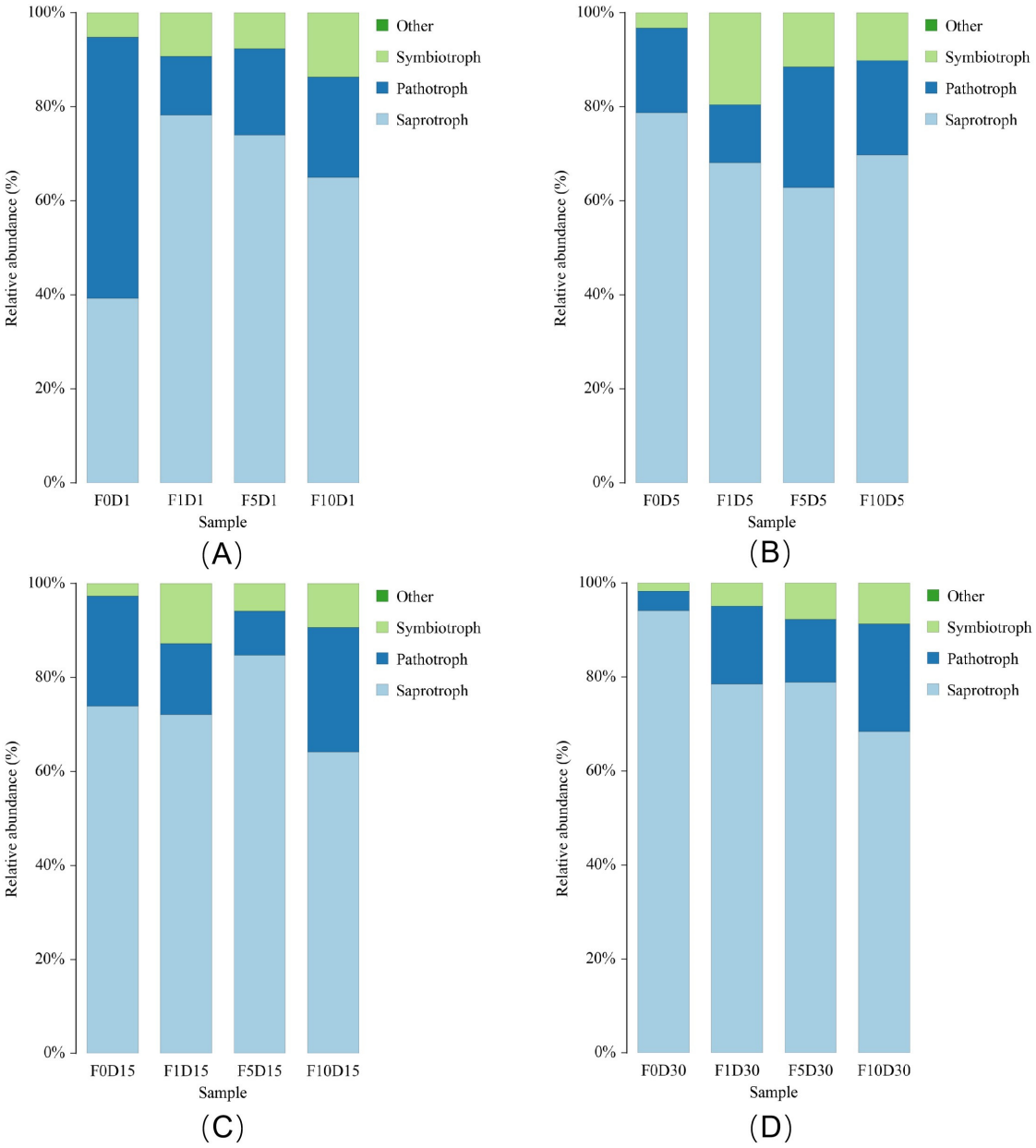

Figure 10. Comparison of relative abundance of fungal saprophytic among different dosage groups with the same treatment duration in soil treatment. (n = 3, $p < 0.05$). Note: (**A**–**D**) represent D1, D5, D15, and D30, respectively.

On the basis of the three broad nutritional modes, the fungal community was further classified into multiple detailed ecological guilds, which served as a finer functional supplement to the trophic mode classification system. Functional guild annotation was conducted using the fungal sequencing data generated in this study, and the results are presented in Figure S6. Compared with the 30-day F0 control (F0D30), the F1 group on day 30 (F1D30) showed significant decreases in three functional guilds, ranked by magnitude of significant difference as follows: coprophilous fungi > unclassified saprotrophic fungi > ectomycorrhizal fungi. Meanwhile, F1D30 exhibited significant increases in four functional guilds, ranked as follows: lichenized fungi > endophytic fungi > plant pathogens > animal pathogens. Compared with F0D30, F5D30 showed a significant decrease only in the guild of unclassified saprotrophic fungi, while the other eight functional guilds increased significantly, ranked by magnitude of difference as follows: wood saprotrophic fungi > plant pathogens > endophytic fungi > animal pathogens > entomopathogenic fungi > coprophilous fungi > ectomycorrhizal fungi. Compared with F0D30, F10D30 showed a significant decrease in the guild of unclassified saprotrophic fungi, while the remaining nine functional guilds increased significantly, ranked as follows: endophytic fungi > animal pathogens > soil saprotrophic fungi > leaf saprotrophic fungi > plant saprotrophic fungi > entomopathogenic fungi > plant pathogens > wood saprotrophic fungi > coprophilous fungi (Figure S7).

3.3.6. Correlation Analysis of Florpyrauxifen-Benzyl Residues with Soil Physicochemical Properties and Fungal Dominant Genera

Environmental factors positively correlated with florpyrauxifen-benzyl residues included air-dried soil moisture content (MC), pH, total potassium (TK) content, and total phosphorus (TP) content, with the strength of positive correlation ranked as follows: MC > pH > TK > TP. Environmental factors negatively correlated with florpyrauxifen-benzyl residues included incubation days (Days), soil organic matter (OM), and total nitrogen (TN) content, with the strength of negative correlation ranked as follows: Days > TN > OM.

The strength of positive correlation with florpyrauxifen-benzyl residues across sample groups was ranked as follows: F10D1 > F10D5 > F10D15 > F5D5 > F5D15 > F5D1 > F1D5 > F10D30. The strength of negative correlation with florpyrauxifen-benzyl residues across sample groups was ranked by correlation coefficient as follows: F1D1 < F0D5 < F0D1 < F5D30 < F1D15 < F0D15 < F0D30 < F1D30.

Fungal genera positively correlated with florpyrauxifen-benzyl residues were ranked by correlation strength as follows: *Aspergillus* > *Phialophora* > *Fusarium* > *Penicillium* > *Chaetomium* > *Mortierella*. The abundance of these genera declined with decreasing florpyrauxifen-benzyl concentration. Fungal genera negatively correlated with florpyrauxifen-benzyl residues were ranked by correlation strength as follows: *Talaromyces* < *Gelasinospora* < *Discosia* < *Botryotrichum*. The abundance of these genera increased with decreasing florpyrauxifen-benzyl concentration (Figure 11).

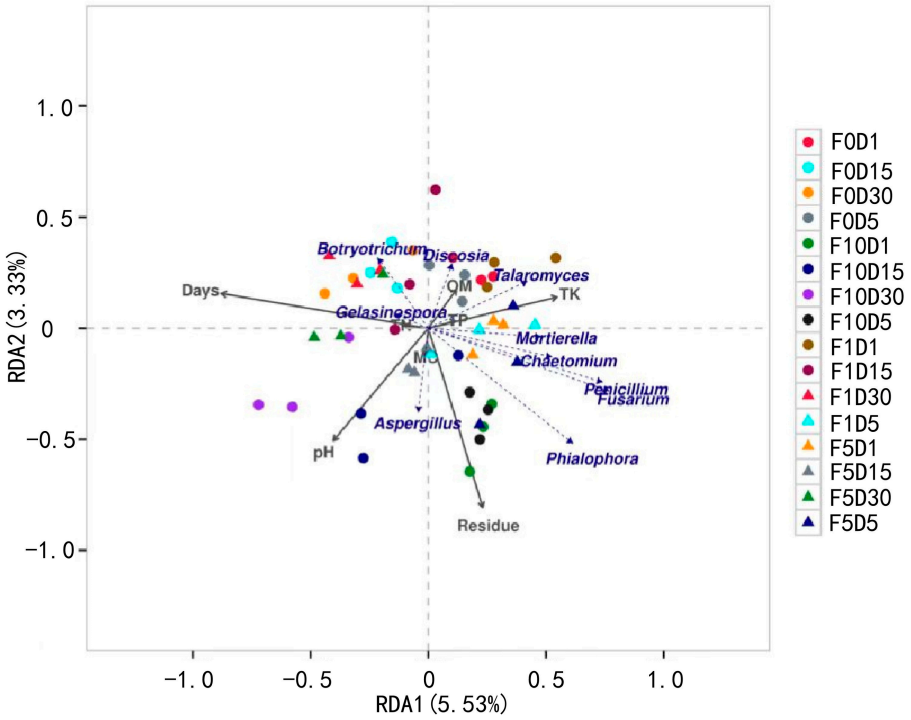

Figure 11. RDA Analysis of Fungal Environmental Factors in Soil Samples. (n = 3, $p < 0.05$). Note: TN: Total Nitrogen; TP: Total Phosphorus; TK: Total Potassium; OM: Organic Matter; MC: Air-Dried Moisture Content; pH: Acidity/Alkalinity; Residue: Florpyrauxifen-benzyl Residue; Days: Treatment Duration.

4. Discussion

4.1. Effects of Florpyrauxifen-Benzyl on Soil Physicochemical Properties

This study tested the hypothesis that the application of florpyrauxifen-benzyl would perturb the physicochemical properties of paddy soil in the pot system. Results from the 30-day pot experiment partially corroborated this hypothesis: following herbicide application, soil total nitrogen, total phosphorus, organic matter, water content, and pH all exhibited fluctuations to varying extents depending on the application rate and sampling time, whereas total potassium showed no significant changes across all treatments and time points. This indicates that the effects of florpyrauxifen-benzyl on soil physicochemical indices are time- and dose-dependent, although not all indices responded to herbicide stress. In the F5 treatment, organic matter significantly decreased and water content significantly increased at later stages; in the high-dose F10 treatment, soil total nitrogen at 15 d and 30 d was significantly elevated compared with the early post-application period. These observations suggest that high-rate florpyrauxifen-benzyl application can drive alterations in certain soil physicochemical parameters within a short-term pot system.

Comparison with other pot simulation studies on similar herbicides revealed that soil ammonium nitrogen following glyphosate applications likewise exhibited temporal fluctuations, without a consistent monotonic increase or decrease pattern [29]. Some studies have reported that soil organic matter content is negatively correlated with herbicide activity [30], which is consistent with our findings. However, long-term field experiments have found that repeated application of certain herbicides can continuously alter soil pH, organic matter pools, and potassium content [31], a finding that differs from our results. These discrepancies may be attributed to differences in experimental duration, soil conditions, and the presence or absence of field environmental processes such as straw incorporation and wetting–drying cycles.

This study revealed correlations between herbicide residues and soil physicochemical properties. Nevertheless, confounding factors in the pot system—such as the release of rice root exudates and inherent soil heterogeneity—may also interfere with the measured physicochemical indices, making it impossible to attribute the observed fluctuations entirely to florpyrauxifen-benzyl application. In subsequent work, a pot control without rice plants will be employed to isolate crop-related interferences and clarify the independent effects of the herbicide.

4.2. Effects of Florpyrauxifen-Benzyl on Soil Fungal Community Structure

This study tested the working hypothesis that the application of florpyrauxifen-benzyl would perturb the community structure and ecological functions of soil fungi in paddy fields. The high-throughput sequencing results supported this hypothesis: fungal α-diversity was significantly elevated in the 5-fold and 10-fold recommended dose groups during the mid-to-late experimental stage (at 15 and 30 days). PERMANOVA revealed no statistically significant differences in overall fungal community composition among groups at the early stages (1 d and 5 d), whereas distinct community divergence occurred among treatments with different application rates at 15 d and 30 d. LEfSe identified a series of time- and dose-dependent indicator species, including *Pseudeurotium bakeri* and *Phialophora cyclaminis*. Genus-level co-occurrence networks indicated that the core network taxa in both the control and herbicide-treated groups underwent turnover over time and with varying doses. FUNGuild functional annotation further demonstrated that the relative abundances of saprotrophic, pathotrophic, and symbiotrophic fungi also exhibited pronounced time- and dose-dependent response patterns. Collectively, these results indicate that the disruptive effect of florpyrauxifen-benzyl on soil fungal communities exhibits a lag effect and dose dependency, with the primary community responses occurring during the mid-to-late stages after application.

In comparison with published studies on similar herbicide–soil fungal interactions, our finding that high-dose treatments elevated fungal α-diversity during the mid-to-late application period has also been reported in soil microcosm experiments with acetochlor and famoxadone, where the proliferation of certain tolerant taxa under high-concentration herbicide stress resulted in increased overall community diversity [32]. Moreover, studies have shown that acetochlor initially inhibits and subsequently promotes soil fungal populations, with the inhibitory and later promotive effects being more pronounced at higher application rates than at lower ones [33]. These results are consistent with the present study, where the fungal diversity indices in the 5-fold and 10-fold dose groups increased significantly at 15 and 30 days. However, some paddy herbicide studies have reported that herbicide treatments reduced fungal diversity [34,35], with the suppressive effects on soil fungi typically occurring during the early post-application period, followed by recovery in later stages due to herbicide degradation and proliferation of tolerant taxa [36]. Such discrepancies may be attributed, on the one hand, to differences in herbicide chemical classes and initial soil microbial community composition, and on the other hand, to the sampling time windows employed. The PERMANOVA results of this study showed that community divergence occurred predominantly during the mid-to-late stages, consistent with the aforementioned "lagged response" pattern. At the community composition level, Ascomycota and Mortierellomycota were the dominant phyla in this study, a pattern consistent with the background community structure reported for most paddy soils in Northeast China [37]. Among the indicator species identified by LEfSe, *Mortierella*, *Phialophora*, and *Fusarium* are also commonly recognized as sensitive or tolerant taxa in herbicide-stressed soils.

Functional annotation of fungi was performed using the FUNGuild database to characterize the functional profiles of soil fungal communities and explore the functional

redundancy within the community. The Glomeraceae family, classified as Symbiotroph, represents typical arbuscular mycorrhizal fungi (AMF), which are widely distributed in paddy soils. This observation is consistent with numerous previous studies investigating fungal communities in rice paddies [38]. Within the Pathotroph guild, genera including *Pseudocercospora*, *Bipolaris*, and *Exserohilum* are well-documented plant pathogens, and their assignment to the Pathotroph guild is in agreement with existing literature [39–41]. For the Saprotroph guild, *Mycena*, *Coprinopsis*, *Penicillium*, and *Aspergillus* are classic *saprotrophic decomposers*, and their guild assignment is supported by prior reports [42–44]. We observed that the relative abundance of some fungal genera decreased concurrently with an increase in other taxa belonging to the same functional guild, which implies a potential compensatory proliferation within the fungal community. Previous research has similarly demonstrated that the taxonomic identities of organisms mediating a given ecosystem function can vary substantially over space or time, while exerting minimal impacts on the overall functional performance of the guild [45].

This study confirmed that florpyrauxifen-benzyl can perturb paddy soil fungal communities in a time- and dose-dependent manner under short-term pot conditions; however, whether this represents a stable community reorganization remains unclear. Future work should include cross-seasonal in situ observations, expand the range of soil types and herbicide concentration gradients, and incorporate metabolites and multiple microbial groups, combined with multi-omics approaches, to further elucidate the complete microecological response mechanisms. In conclusion, florpyrauxifen-benzyl perturbs paddy soil fungal communities in a time- and dose-dependent manner under short-term pot conditions; nevertheless, the long-term soil ecological risks of this herbicide still require further validation through more in situ field experiments across diverse soil types and extended temporal scales.

5. Conclusions

Residues of florpyrauxifen-benzyl in potted rice soil, applied at the recommended rate as well as 5-fold and 10-fold the recommended rate, followed a negative exponential decay function. It was confirmed that elevated application rates of florpyrauxifen-benzyl exerted significant effects on soil fungal community structure. Compared with the untreated control, the abundances of *Pseudeurotium bakeri* and *Phialophora cyclaminis* in the 10-fold dose group increased significantly on days 5 and 15, respectively. Relative to both the control and the recommended-rate group, the fungal diversity indices in the 5-fold and 10-fold dose groups were significantly higher on days 15 and 30. On the first day after application, the composition of the core fungal microbiota differed markedly between the herbicide-treated groups and the control. The effects of different application rates on the abundance of soil fungal trophic guilds varied over time: compared with the control, Saprotrophic abundance increased on day 0 (the day of application) but decreased on days 15 and 30; Pathotrophic abundance decreased across three time points from day 1 to day 15; and Symbiotrophic abundance increased significantly across four time points from day 1 to day 30. These findings provide a theoretical basis for elucidating the disturbance pattern of florpyrauxifen-benzyl to soil fungi, mitigating soil-borne crop root diseases, and preventing soil microecological imbalance.

Supplementary Materials: The following supporting information can be downloaded at: https://www.mdpi.com/article/10.3390/d18090576/s1. Table S1 the specific dissipation kinetic parameters of florpyrauxifen-benzyl in soil.; Table S2. Changes in soil physicochemical properties of each treatment group over time.; Figure S1. shows bar charts of the changes in soil physicochemical properties over time for each treatment group.; Figure S2. Heatmap illustrating the hierarchical clustering of the top 30 species-level abundances in soil samples.; Figure S3. Alpha diversity analysis curves

of the samples.; Figure S4. Circle-based correlation network diagram.; Figure S5.COG metabolic pathway histogram.; Figure S6. Comparison of relative abundance of fungal nutritional types over time after soil application of fungicide.; Figure S7. Guild Classification Statistical Group Functional Difference Bar Chart.

Author Contributions: C.L.: Conceptualization, Data curation, Formal analysis, Software, Visualization, Writing—original draft. B.T.: Project administration, Resources, Supervision, Writing—review & editing. Z.Z.: Formal analysis, Investigation, Software, Visualization Investigation, Methodology. H.F.: Investigation, Project administration. X.S.: Data curation, Validation. F.Y.: Conceptualization, Funding acquisition, Methodology, Supervision, Writing—review & editing. All authors have read and agreed to the published version of the manuscript.

Funding: This study was financially supported by the Heilongjiang University Special Fund Project under the Basic Scientific Research Operating Expenses for Universities in Heilongjiang Province (2025-KYYWF-ZR0370).

Data Availability Statement: Data will be made available on request.

Acknowledgments: The authors have reviewed and edited the output and take full responsibility for the content of this publication.

Conflicts of Interest: The authors declare no conflicts of interest.

References

1. Miller, M.; Norsworthy, J. Influence of soil moisture on absorption, translocation, and metabolism of florpyrauxifen-benzyl. *Weed Sci.* **2018**, *66*, 418–423. [CrossRef]
2. Tu, W.M.; Ma, Y.N.; Pan, J.Y.; Huang, S.Q.; Chen, M.X. Identification of hydrolysis products of florpyrauxifen-benzyl and establishment of its detection method. *Qual. Saf. Agric. Prod.* **2021**, *3*, 40–48. (In Chinese)
3. Zhou, R.D.; Dong, Z.M.; Zhao, W.N.; Bian, C.F.; Gao, M.Z.; Liu, L.; Wu, T.Q.; Li, B.T. Determination of 3% florpyrauxifen-benzyl emulsifiable concentrate by ultra-performance liquid chromatography-quadrupole linear ion trap-time-of-flight mass spectrometry. *Pesticides* **2022**, *61*, 496–499. (In Chinese)
4. Bhardwaj, L.; Reddy, B.; Dubey, S.K. Deciphering insights into rhizospheric microbial community and soil parameters under the influence of herbicides in zero-tillage tropical rice-agroecosystem. *Environ. Res.* **2023**, *237*, 117033. [CrossRef] [PubMed]
5. Du, P.; He, H.; Wu, X.; Xu, J.; Dong, F.; Liu, X.; Zheng, Y. Mesosulfuron-methyl influenced biodegradability potential and N transformation of soil. *J. Hazard. Mater.* **2021**, *416*, 125770. [CrossRef] [PubMed]
6. Liu, Y.; Fan, X.; Zhang, T.; Sui, X.; Song, F. Effects of atrazine application on soil aggregates, soil organic carbon and glomalin-related soil protein. *Plant Soil Environ.* **2021**, *67*, 173–181. [CrossRef]
7. Chávez-Ortiz, P.; Tapia-Torres, Y.; Larsen, J.; García-Oliva, F. Glyphosate-based herbicides alter soil carbon and phosphorus dynamics and microbial activity. *Appl. Soil Ecol.* **2022**, *169*, 104256. [CrossRef]
8. Zhou, T.T. Effects of Two Typical Pesticides on Soil Microbial Community Composition, Function and Structure. Master's Thesis, Shandong Agricultural University, Tai'an, China, 2021.
9. Ma, Q.; Tan, H.; Song, J.; Li, M.; Wang, Z.; Parales, R.E.; Li, L.; Ruan, Z. Effects of long-term exposure to the herbicide nicosulfuron on the bacterial community structure in a factory field. *Environ. Pollut.* **2022**, *307*, 119477. [CrossRef] [PubMed]
10. Ghosh, D.; Roy, K.; Srinivasan, V.; Mueller, T.; Tuovinen, O.H.; Sublette, K.; Peacock, A.; Radosevich, M. In-situ enrichment and analysis of atrazine-degrading microbial communities using atrazine containing porous beads. *Soil Biol. Biochem.* **2009**, *41*, 1331–1334. [CrossRef]
11. Lv, Z.; Su, A.; Hu, F.Y.; Ding, Z.M.; Wang, B.Y.; Xu, M.K.; Zhang, H.W.; An, J. Effects of Sesbania on chlorimuron-ethyl removal and soil microbial communities in farmland. *Chin. J. Ecol.* **2024**, *43*, 2750–2757.
12. Kusumavathi, K.; Sarkar, S.; Ali, A.; Bera, S.; Krishna, V.V.S.J.; Maity, S.; Devi, N.M.; Bandopadhyay, P. Effect of diverse crop establishment techniques and weed management approaches in rice-chickpea cropping systems on soil attributes. *BMC Plant Biol.* **2025**, *25*, 372. [CrossRef] [PubMed]
13. Duque, T.S.; Pinheiro, R.A.; Souza, I.M.; Silva, G.G.; Soares, M.A.; dos Santos, J.B. Herbicides and bio-inputs: Compatibility and challenges for sustainable agriculture. *Chemosphere* **2024**, *369*, 143878. [CrossRef] [PubMed]
14. Yuan, M.; Yang, F.; Wang, P.; Fu, H.; Ge, Z.; Zhang, Z.; Liu, C. Effect of Florpyrauxifen-Benzyl on Methane-Metabolizing Microbial Community in Rice Rhizosphere Soil. *Microorganisms* **2026**, *14*, 1228. [CrossRef] [PubMed]
15. Yang, X.; Lai, J.L.; Zhang, Y.; Luo, X.G.; Han, M.W.; Zhao, S.P. Microbial community structure and metabolome profiling characteristics of soil contaminated by TNT, RDX, and HMX. *Environ. Pollut.* **2021**, *285*, 117478. [CrossRef] [PubMed]

16. Sheetal, M.; Patil, V.B.; Madhavi, P. A validated stability-indicating method for separation of prucalopride drug by HPLC: Method transfer to UPLC. *Anal. Chem. Lett.* **2021**, *11*, 1911680. [CrossRef]
17. Wang, L.; Wang, L.; Zhan, X.Y.; Huang, Y.K.; Wang, J.; Wang, X. Response mechanism of microbial community to the environmental stress caused by the different mercury concentration in soils. *Ecotoxicol. Environ. Saf.* **2020**, *188*, 109906. [CrossRef] [PubMed]
18. Sun, Y.; Shi, Y.; Tang, Y.; Tian, J.; Wu, X. Correlation between plant diversity and the physicochemical properties of soil microbes. *Appl. Ecol. Environ. Res.* **2019**, *17*, 10371–10388. [CrossRef]
19. Bao, S.D. Determination of soil nitrogen content by sulfuric acid digestion-Kjeldahl method. In *Soil and Agricultural Chemistry Analysis*; China Agricultural Press: Beijing, China, 2000; pp. 42–56. (In Chinese)
20. Bao, S.D. Determination of soil phosphorus content by sodium hydroxide fusion and molybdenum-antimony ascorbic acid colorimetric method. In *Soil and Agricultural Chemistry Analysis*; China Agricultural Press: Beijing, China, 2000; pp. 76–80. (In Chinese)
21. Bao, S.D. Determination of total potassium content in soil by flame photometry. In *Soil and Agricultural Chemistry Analysis*; China Agricultural Press: Beijing, China, 2000; pp. 270–271. (In Chinese)
22. Ministry of Agriculture of the People's Republic of China. Determination of soil organic matter (organic carbon) by potassium dichromate volumetric method—External heating method: NY/T 1121.6-2006. In *Soil Testing—Part 6: Determination of Soil Organic Matter*; Ministry of Agriculture of the People's Republic of China: Beijing, China, 2006.
23. Edgar, R.C.; Haas, B.J.; Clemente, J.C.; Quince, C.; Knight, R. UCHIME improves sensitivity and speed of chimera detection. *Bioinformatics* **2011**, *27*, 2194–2200. [CrossRef] [PubMed]
24. Edgar, R.C. UPARSE: Highly accurate OTU sequences from microbial amplicon reads. *Nat. Methods* **2013**, *10*, 996–998. [CrossRef] [PubMed]
25. Bokulich, N.A.; Subramanian, S.; Faith, J.J.; Gevers, D.; Gordon, J.I.; Knight, R.; Mills, D.A.; Caporaso, J.G. Quality-filtering vastly improves diversity estimates from Illumina amplicon sequencing. *Nat. Methods* **2013**, *10*, 57–59. [CrossRef] [PubMed]
26. Callahan, B.J.; Mcmurdie, P.J.; Rosen, M.J.; Han, A.W.; Johnson, A.J.A.; Holmes, S.P. DADA2: High-resolution sample inference from Illumina amplicon data. *Nat. Methods* **2016**, *13*, 581–583. [CrossRef] [PubMed]
27. Marti, J.A. A new method for non-parametric multivariate analysis of variance. *Austral Ecol.* **2001**, *26*, 32–46. [CrossRef]
28. Nguyen, N.H.; Song, Z.W.; Scott, T.; Bates, S.T. FUNGuild: An open annotation tool for parsing fungal community datasets by ecological guild. *Fungal Ecol.* **2016**, *20*, 241–248. [CrossRef]
29. Li, P.; Zhai, W.; Li, B.; Guo, Q.; Wang, Y.; Gu, Y.; Zheng, L.; Zhao, F.; Liu, X.; Wang, P.; et al. Glyphosate and urea co-exposure: Impacts on soil nitrogen cycling. *J. Hazard. Mater.* **2025**, *492*, 138150. [CrossRef] [PubMed]
30. Grey, T.L.; McCullough, P.E. Sulfonylurea Herbicides' Fate in Soil: Dissipation, Mobility, and Other Processes. *Weed Technol.* **2013**, *26*, 579–581. [CrossRef]
31. Meng, P.; Huang, C.; Song, H.; Shen, Z.; Zhang, B.; Yan, J.; Yu, M.; Guo, L. Long-term glyphosate application impairs peach (Prunus persica) tree growth by altering soil microbial communities and nutrient availability. *Plant Soil* **2026**, *520*, 841–858. [CrossRef]
32. Li, X.; Zhang, H.; Wu, M.; Zhang, Y.; Zhang, C. Effect of methamidophos on soil fungi community in microcosms by plate count, DGGE and clone library analysis. *Environ. Sci.* **2008**, *20*, 619–625. [CrossRef] [PubMed]
33. Jing, R.Y.; Wang, L.Y.; Wang, Y.J.; Tan, H.B.; Mu, G.Q.; Wang, W.D. Effects of acetochlor on soil microbial population and enzyme activities. *Chin. J. Eco-Agric.* **2010**, *18*, 1302–1305. (In Chinese) [CrossRef]
34. Romero, F.; Jiao, S.; van der Heijden, M.G. Impact of microbial diversity and pesticide application on plant growth, litter decomposition and carbon substrate use. *Soil Biol. Biochem.* **2025**, *208*, 109866. [CrossRef]
35. European Commission. *Renewal Report for the Active Substance Glyphosate*; Document PLAN/2023/1497 RR-Rev. 1; European Commission: Brussels, Belgium, 2023.
36. Tu, C.M. Effetc of fungicides, captafol and chlorothalonil, on microbial and enzymatic-activities in mineral soil. *Environ. Sci.* **1993**, *28*, 67–80. [CrossRef] [PubMed]
37. Li, H.Y.; Zhang, G.L.; Fan, M.Y.; Zheng, G.P.; Lv, Y.D. Effects of continuous biochar amendment on nutrients and fungal community structure of soda-saline paddy soil. *J. Soil Water Conserv.* **2020**, *34*, 345–351. (In Chinese)
38. Senapati, A.; Panneerselvam, P.; Chidambaranathan, P.; Nayak, A.K.; Mitra, D.; Pradhan, C.; Anandan, A. Ecological dynamics of Arbuscular Mycorrhizal Fungi in wetland and aerobic rice ecosystem under subtropical humid climatic conditions in Eastern India. *Symbiosis* **2024**, *93*, 99–113. [CrossRef]
39. Świderska-Burek, U.; Daub, M.E.; Thomas, E.; Jaszek, M.; Pawlik, A.; Janusz, G. Phytopathogenic Cercosporoid Fungi—From Taxonomy to Modern Biochemistry and Molecular Biology. *Int. J. Mol. Sci.* **2020**, *21*, 8555. [CrossRef] [PubMed]
40. Yan, R.; Zhou, X.Y.; Zhang, J.G.; Wang, L.; Li, J.; Liang, J.; Gong, J.Y.; Du, Y.; Li, K.M.; Lei, B. Pathogen identification and biological characteristics of Bipolaris sorokiniana causing wheat root rot in Xinjiang. *Xinjiang Agric. Sci.* **2024**, *61*, 1209–1217. (In Chinese)
41. Nsibo, D.L.; Barnes, I.; Berger, D.K. Recent advances in the population biology and management of maize foliar fungal pathogens Exserohilum turcicum, Cercospora zeina and Bipolaris maydis in Africa. *Front. Plant Sci.* **2024**, *15*, 1404483. [CrossRef] [PubMed]

42. Ghosh, A.; Frankland, J.C.; Thurston, C.F.; Robinson, C.H. Enzyme production by Mycena galopus mycelium in artificial media and in Picea sitchensis F1 horizon needle litter. *Mycol. Res.* **2003**, *107*, 996–1008. [CrossRef] [PubMed]
43. Nakazawa, T.; Izuno, A.; Horii, M.; Kodera, R.; Nishimura, H.; Hirayama, Y.; Tsunematsu, Y.; Miyazaki, Y.; Awano, T.; Muraguchi, H.; et al. Effects of pex1 disruption on wood lignin biodegradation, fruiting development and the utilization of carbon sources in the white-rot Agaricomycete Pleurotus ostreatus and non-wood decaying Coprinopsis cinerea. *Fungal Genet. Biol.* **2017**, *109*, 7–19. [CrossRef] [PubMed]
44. Akpasi, S.O.; Anekwe, I.M.S.; Tetteh, E.K.; Amune, U.O.; Shoyiga, H.O.; Mahlangu, T.P.; Kiambi, S.L. Mycoremediation as a Potentially Promising Technology: Current Status and Prospects—A Review. *Appl. Sci.* **2023**, *13*, 4978. [CrossRef]
45. Louca, S.; Polz, M.F.; Mazel, F.; Albright, M.B.; Huber, J.A.; O'Connor, M.I.; Ackermann, M.; Hahn, A.S.; Srivastava, D.S.; Crowe, S.A.; et al. Function and functional redundancy in microbial systems. *Nat. Ecol. Evol.* **2018**, *2*, 936–943. [CrossRef] [PubMed]